Available online at www.sciencedirect.com
ScienceDirect
Developmental Biology 307 (2007) 14–28
DEVELOPMENTAL BIOLOGY
www.elsevier.com/locate/ydbio

Neurturin-GFRα2 signaling controls liver bud migration along the ductus venosus in the chick embryo

Norifumi Tatsumi, Rika Miki, Kenjiro Katsu, Yuji Yokouchi *

Division of Pattern Formation, Department of Organogenesis, Institute of Molecular Embryology and Genetics, Kumamoto University, 2-2-1 Honjo, Kumamoto 860-0811, Japan
The 21st Century COE 'Cell Fate Regulation Research and Education Unit,' Kumamoto University, Japan

Received for publication 29 May 2006; revised 28 February 2007; accepted 27 March 2007
Available online 3 April 2007

Abstract

During chick liver development, the liver bud arises from the foregut, invaginates into the septum transversum, and elongates along and envelops the ductus venosus. However, the mechanism of liver bud migration is only poorly understood. Here, we demonstrate that a GDNF family ligand involved in neuronal outgrowth and migration, neurturin (NRTN), and its receptor, GFRα2, are essential for liver bud migration. In the chick embryo, we found that *GFRα2* was expressed in the liver bud and that *NRTN* was expressed in the endothelial cells of the ductus venosus. Inhibition of GFRα2 signaling suppressed liver bud elongation along the ductus venous without affecting cell proliferation and apoptosis. Moreover, ectopic expression of *NRTN* perturbed the directional migration along the ductus venosus, leading to splitting or ectopic branching of the liver. We showed that liver buds selectively migrated toward an NRTN-soaked bead *in vitro*. These data represent a new model for liver bud migration: NRTN secreted from endothelial cells functions as a chemoattractant to direct the migration of the GFRα2-expressing liver bud in early liver development.

Keywords: Liver development; GDNF; Neurturin; Migration; Chick; Organogenesis; Endoderm; Chemoattractant; Ductus venosus; Endothelial cell

Introduction

The vertebrate liver is a metabolic organ comprised largely of hepatic parenchyma, biliary tracts, and sinusoids which serve to metabolize chemicals, transport the bile from the parenchyma, and transport venous blood from the portal vein, respectively. Liver originates in the hepatic endoderm, which arises from the anterior intestinal portal in response to inductive signals emanating from the neighboring mesoderm-derived tissues (Lemaigre and Zaret, 2004; Le Douarin, 1975). These signals include FGFs from the cardiac mesoderm and BMP4 from the septum transversum mesenchyme (STM) (Jung et al., 1999; Rossi et al., 2001). Following hepatic induction, the hepatic endoderm induced in the ventral foregut invaginates into the STM to form the liver bud. Following invagination, the liver bud undergoes morphogenesis in a species-specific manner. In the case of the mouse embryo, the basement membrane degrades around the liver bud and then the liver bud interacts with primitive endothelial cells (ECs) in the loose mesenchyme at E9.5. The hepatoblasts derived from the bud migrate into the STM and intermingle with mesenchymal cells and ECs to form hepatocellular cords (Hentsch et al., 1996; Sosa-Pineda et al., 2000; Matsumoto et al., 2001; Zhao and Duncan, 2005). This interaction triggers outgrowth of the liver bud and the vitelline vein and umbilical veins are incorporated into the liver after E10. These veins are subsequently remodeled into the ductus venosus (Zaret, 1996; Hentsch et al., 1996; Kaufman and Bard, 1999). In contrast, morphogenesis of the chick liver bud appears to require the interaction of the liver bud with the ductus venosus. The ductus venosus is formed in the liver by the union of the left and right vitelline vein. The ductus venosus ends at the junction with the sinus venosus, a horn receiving blood from the ductus venosus and ducts of

* Corresponding author. Fax: +81 96 373 6625.
E-mail address: yokouchi@kaiju.medic.kumamoto-u.ac.jp (Y. Yokouchi).

0012-1606/$ - see front matter © 2007 Elsevier Inc. All rights reserved.
doi:10.1016/j.ydbio.2007.03.519

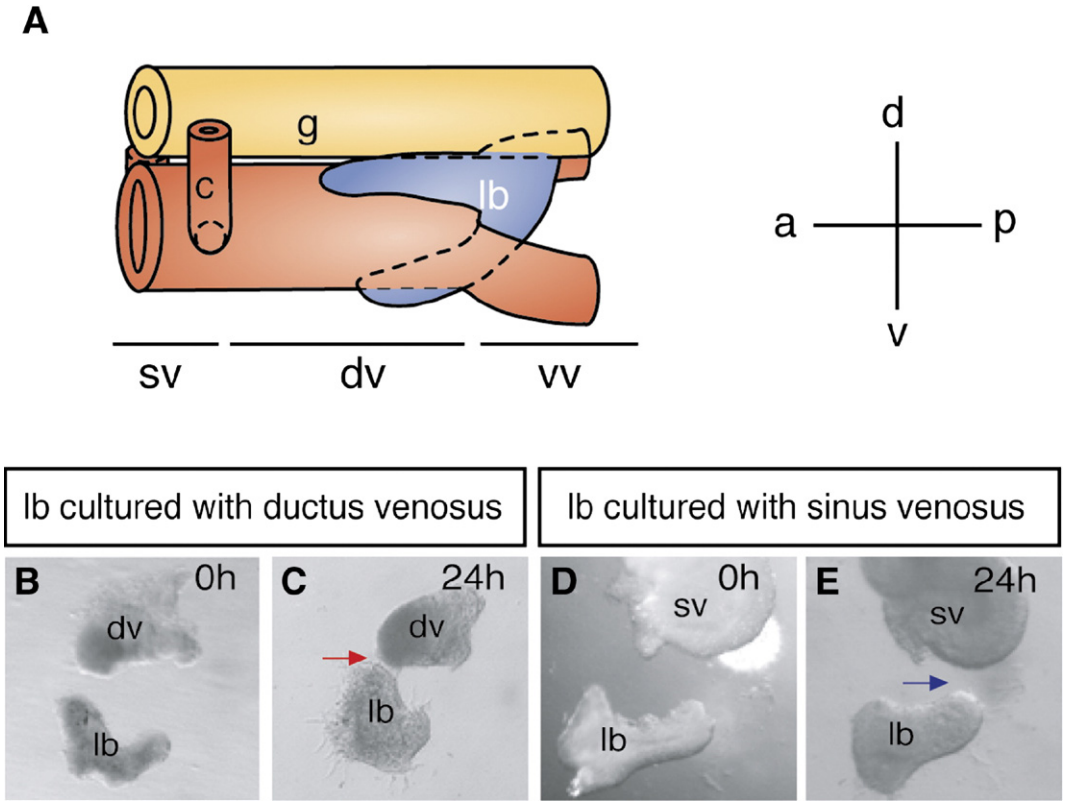

Fig. 1. Explants of ductus venosus promote the migration of liver buds *in vitro*. (A) Scheme showing the spatial relationship between the gut (g), liver bud (lb), and the veins in the chick embryo during HH16–17. Along the anterior–posterior axis, the vein (red) is subdivided into the sinus venous (sv), the ductus venosus (dv), and the vitelline veins (vv). During these stages, the two diverticula of the liver bud (blue) invaginated from the foregut endoderm migrate anteriorly on the dorsal or ventral side of the ductus venosus. The orientation compass shows anterior (a), posterior (p), dorsal (d) and ventral (v) orientation. c, Duct of Cuvier. (B–E) Co-cultures of liver bud with the ductus venosus or the sinus venosus. Isolated liver bud from HH16 chick embryos was cultured in type I collagen gel with an explant of the ductus venosus (B, C) or the sinus venosus (D, E) for 24 h. The red arrow in panel C shows the liver bud migrating toward the ductus venosus. The blue arrow in panel E shows the gap between the liver bud and the sinus venosus.

Cuvier (please see Fig. 1A). After invagination, the liver buds first elongate forward along the ductus venosus (HH15–17), then extend laterally on and envelop the ductus venosus (HH17–21), and finally proliferate radially to form hepatocellular cords in the STM (Romanoff, 1960; Le Douarin, 1975; reviewed in Yokouchi, 2005). Although the morphogenetic processes in the mouse and chick STM clearly differ, the migration of mouse and chick liver buds appears to depend on interactions between hepatoblasts of the liver bud and ECs in the STM.

Mutational analyses performed in the mouse have provided evidence in favor of a role for ECs in the STM in the morphogenetic processes leading to the migration of the liver bud in the embryo. In the null mutant of *Flk-1* (VEGFR-2), a cell surface receptor for vascular endothelial growth factor (VEGF), the formation of *Flk-1*-positive ECs surrounding the liver bud is suppressed, and the delamination and migration of the liver bud is secondarily inhibited *in vivo* (Matsumoto et al., 2001). In addition, loss-of-function analysis revealed that a homeobox transcription factor *Prox1*, which is expressed in the vertebrate liver bud and pancreatic buds (Burke and Oliver, 2002; Liu et al., 2003; Yanai et al., 2005), is required for this migration process in the mouse embryo (Sosa-Pineda et al., 2000). Despite our recent understanding of the contribution of *Flk-1* and *Prox1* to the control of the migration of the liver buds, little is known of which secreted proteins directly regulate liver bud migration.

Glial-cell-line-derived neurotrophic factor (GDNF) and the related GDNF family ligands (GFLs), neurturin (NRTN), artemin (ARTN) and persephin (PSPN), belong to the TGF-β superfamily. These proteins are neurotrophic factors for neurons and attractive guidance signals for sensory and sympathetic axons (Airaksinen and Saarma, 2002; Ledda et al., 2002). In addition, GDNF and the related ligand, NRTN, are chemoattractants for enteric neural crest-derived cells, and promote the migration of vagal neural crest cells into and along the gastrointestinal tract (Yan et al., 2004).

Generally, all GFLs share the receptor tyrosine kinase RET as a common signaling receptor. The ligand-binding specificity of GFLs is determined by GFRα proteins, which are GPI-anchored extracellular proteins with unique binding affinities for each GFL. GDNF, NRTN, ARTN and PSPN specifically bind to GFRα1, GFRα2, GFRα3 and GFRα4, respectively. The homodimeric GFLs first form a high-affinity complex with one of the four GFRα proteins. The GFL-GFRα complex brings two molecules of RET together, triggering transphosphorylation of specific tyrosine residues in the tyrosine kinase domains and intracellular signaling (Airaksinen and Saarma, 2002). In addition, several studies have shown that there is a RET-

independent component to GFL signaling involving neural cell adhesion molecule (NCAM) (Paratcha et al., 2003).

Recently, analysis of the expression of GFLs and their receptors in chick embryo revealed strong expression of *GFRα2* in the liver (Homma et al., 2000). Expression of *NRTN*, a preferred ligand for GFRα2, has been detected in the hepatic sinusoids of the mouse embryonic liver (Golden et al., 1999). Moreover, recent studies demonstrate that, outside the nervous system, axon guidance cues mediated by factors such as GFLs play diverse roles in the generation of complex tissues such as the lung, mammary gland, cardiovasculature, spermatogonia, and kidney (Hinck, 2004; Sariola and Saarma, 2003). This evidence suggests that NRTN-GFRα2 signaling might be involved in the development of the liver.

In this study, we examined both the detailed expression pattern and signaling functions of *NRTN-GFRα2* in the morphogenesis of chick embryonic liver. We show that *NRTN* is expressed in the ECs of the ductus venosus and that its receptor *GFRα2* is expressed in the migrating liver bud on the ductus venosus. We also observed that inhibition of the binding of NRTN to endogenous GFRα2 by the expression of a soluble *GFRα2* repressed the anterior elongation of the liver bud. In addition, the ectopic expression of *NRTN* in the prospective hepatic endoderm prevented the liver bud from enveloping the ductus venosus. Moreover, similar ectopic expression of *NRTN* in the prospective midgut endoderm induced the formation of an ectopic branch of the liver in the duodenum due to erroneous liver bud migration. We also observed that isolated liver bud selectively migrates toward an NRTN-soaked bead *in vitro*. Taken together, our data indicate that NRTN is a chemoattractant essential for the migration of the chick liver bud expressing of the corresponding receptor, GFRα2 in early chick liver development.

Materials and methods

Animals

Fertilized chicken eggs (White Leghorn, Setoguchi Hatchery, Kumamoto, Japan) were incubated at 38 °C and the embryos were staged according to Hamburger and Hamilton (1951). We used E9.5 mouse embryos from pregnant mice of the ICR strain (Charles River Laboratories Japan Inc., Kanagawa, Japan).

Isolation of cDNAs encoding chick GFRα1, GFRα2 and GFRα4, and mouse GDNF and NRTN

Total RNA was isolated from chick embryos at embryonic day 4 (E4) and from 9.5-day-old mouse embryos using TRIzol Reagent (Invitrogen). First-strand cDNA was reverse transcribed from this RNA using the SuperScript™ Preamplification System (GIBCO BRL). cDNAs for chick *GFRα1* (Genbank accession no. U90541), *GFRα2* (Genbank accession no. U90542), *GFRα4* (Genbank accession no. AF045162), *mGNDF* (Genbank accession no. NM_010275), and *mNRTN* (Genbank accession no. NM_008738) were amplified by polymerase chain reaction (PCR) using Platinum *Pfx* DNA polymerase (Invitrogen) and then ligated into pSLAX-21 and sequenced.

Cloning, library screening and sequencing of chick NRTN

Degenerate primers NRTN-A and NRTN-B were designed that recognize sequences corresponding to a processed, mature domain that is highly conserved at the amino acid level among the known vertebrate NRTNs and chick GDNF: primer NRTN-A, 5′-TGAG(C/T) GA (A/G)(C/T) TGGG (A/C/G/T)(C/T) TGGG (A/C/G/T) TAC-3′; primer NRTN-B, 5′-GA (A/C/G/T) AG(C/T) TC (C/T) TGCAG (A/C/G/T) GTGTGGTA-3′. PCR was performed using the following conditions: 95 °C for 1 min, 55 °C for 1 min, and 72 °C for 1 min for 40 cycles using FastStart Taq DNA Polymerase (Roche). PCR products of the expected size (180 bp) were ligated into pGEM-T Easy Vector (Promega). Several clones were sequenced using the ABI 310 automated sequencer and these were found to contain the expected fragment of the chick *NRTN* gene. To obtain a full-length cDNA, a 4- to 10-day chick liver cDNA library was screened using the PCR fragment as a probe. Hybridization under high-stringent conditions allowed the isolation of eight independent clones and one clone contained the entire open reading frame of *NRTN*.

In situ hybridization and probes

Whole-mount *in situ* hybridization was performed as previously described (Riddle et al., 1993). Plasmids containing the genes for chick *hhex*, *fibrinogen-γ*, *transthyretin*, *Foxa2* and *Prox1* (Yanai et al., 2005), chick *GFRα1*, *GFRα2*, and *GDNF* (kind gifts from Dr. S. Homma), and chick *c-ret* (a kind gift from Dr. F. Costantini) were used to make antisense probes as previously described (Yanai et al., 2005; Homma et al., 2000; Schuchardt et al., 1995). Antisense probes for chick *GFRα4* and *NRTN* were synthesized using T3 RNA polymerase from a template linearized with *Nco*I for *GFRα4* and *Eco*RI for *NRTN*.

Plasmid construction

To construct soluble forms of GFRα1 (GFRα1-Fc) and GFRα2 (GFRα2-Fc), the GPI anchoring site was deleted by PCR. The cDNA regions of GFRα1 corresponding to the sequences 623 bp–1281 bp and GFRα2 at 438–1326 were amplified by PCR using the following primers: 5′-ATGCTCTT-CTGCTCCTGTCGAG-3′ and 5′-CTCGAGGGCCAGAACGACTC-CTGGTGTGTT-3′ for GFRα1ΔGPI, 5′-ATCTCCACCTGCAGCAAGGAG-3′ and 5′-CTCGAGGGCCAGAACTGCCTTCTGATCCAC-3′ for GFRα2ΔGPI. An *Xho*I site (underlined) was incorporated at the 5′ end of each reverse primer for recombination in-frame to the Fc fragment. The resulting products were cloned, digested with *Nde*I or *Bgl*II and inserted into the *Nde*I/*Bam*HI sites of pSLAX-GFRα1 or the *Bgl*II/*Eco*RI sites of pSLAX-GFRα2 (pSLAX-GFRα1ΔGPI and pSLAX-GFRα2ΔGPI). The cDNA fragment encoding the Fc domain of mouse IgG was excised from La518Fc vector (kind gift from W.J. LaRochelle) (LaRochelle et al., 1995) with *Xho*I/*Bam*HI and inserted into the *Xho*I/*Bam*HI sites of pSLAX-GFRα1ΔGPI and pSLAX-GFRα2ΔGPI (pSLAX-GFRα1-Fc and pSLAX-GFRα2-Fc). The inserts of all constructs were confirmed by sequence analysis. The fragments encoding GFRα1-Fc and GFRα2-Fc were subcloned into the pCAGGS expression vector (Niwa et al., 1991). The open reading frames of mGDNF and mNRTN were amplified by PCR and inserted into a version of pSlax13 vector to generate mGDNF and mNRTN carrying a 3× HA epitope at the carboxy-terminus (Laufer et al., 1997). The HA-tagged mGDNF and mNRTN were excised and cloned into the pCAGGS vector.

Electroporation and ex ovo culture of whole embryo

The transgene was specifically electroporated into the endodermal layer of the chick embryo and cultured using the method of Flamme (1987). HH11–12 chick embryos were explanted using a ring of filter paper and yolk was removed completely by washing with PBS. The embryos were positioned with their ventral side facing the negative electrode. The DNA solution was placed on the target region, according to the fate map (Matsushita, 1999), and then the embryos were subjected to electroporation. Electroporation was carried out using four electric pulses of 6 V, for 25 ms with a CUY21 electroporator (Tokiwa Science, Japan). In all experiments, the final concentration of DNA was adjusted to 5.0 μg/μl, and that of pCAGGS-GFP to 1.0 μg/μl. After electroporation, embryos were immediately washed in PBS. The paper ring with the embryo was set on a culture apparatus that had been prepared as follows. Stainless steel rings were affixed to the bottoms of 6-cm petri dishes with silicon grease (Dow

Corning). The inside of the ring was then filled with culture medium containing yolk and albumen (2:1), and penicillin/streptomycin (Gibco). Embryos were cultured at 38 °C for 24 or 48 h in a humidified incubator.

Immunohistochemistry

Embryos were fixed in 4% paraformaldehyde (PFA)/PBS for 2 h, and then equilibrated in 30% sucrose/PBS overnight for cryoprotection. The embryos were embedded in Tissue Tek OCT compound and frozen. Ten-micrometer cryosections were cut in a cryostat (Leica) and post-fixed in acetone. Slides were washed in 0.1% (v/v) Triton X-100/TBS with 10 mM $CaCl_2$, or 0.1%(v/v) Triton X-100/PBS and blocked for 30 min in 5% normal goat serum. The following primary antibodies were used: mouse anti-E-cadherin (BD 1:300), rabbit anti-laminin (SIGMA 1:100) and mouse anti-GFP (SIGMA 1:500). Primary antibody treatments were applied for 1 h or overnight in a humidified chamber at 4 °C. Binding of the primary antibodies was detected using the following fluorescent secondary antibodies: Fluorolink Cy3-labeled goat anti-mouse IgG (Amersham Biosciences 1:300), Alexa Fluor 488 goat anti-rabbit IgG (Molecular Probes 1:300), Fluorolink Cy3-labeled goat anti-rabbit IgG (Amersham Biosciences 1:300) and Alexa Fluor 488 goat anti-mouse IgG (Molecular Probes 1:300). Fluorescent secondary antibodies were applied for 1 h at room temperature.

Cell proliferation and apoptosis (TUNEL) assays

Frozen sections were prepared as described above. Adjacent sections of each specimen were collected and used for assays of cell proliferation and apoptosis. Cell proliferation was assessed by immunohistochemistry with anti-phosphohistone H3 (Ser10) (SIGMA 1:500). Apoptosis was assessed by the TUNEL technique (ApopTag, Molecular Probes). After these procedures, the specimens were stained with DAPI (Nakarai) to count cell numbers. Serial sections through the entire liver bud were examined and the sections with the largest numbers of positive cells were used for quantification. The number of phosphohistone H3- or TUNEL-positive cells/liver bud cells was counted in four embryos transduced with pCAGGS-GFRα2-Fc and three control embryos. The data were analyzed statistically using the Student's *t*-test and significance was set at $p=0.05$.

Explant culture

For explant culture, we modified the method of Nogawa and Ito (1995) and established by Yanai (unpublished). Briefly, isolated liver buds from HH16–17 chick embryos were treated with 0.25 mg/ml collagenase (WOR) to remove the mesenchymes and the vein from the hepatic diverticula. A 10 μl drop of type I collagen gel (Nitta Gelatin) was transferred by pipette into a culture dish (Wako) and allowed to polymerize at 38 °C for 10 min. Tissue or protein-soaked beads were transferred onto this collagen drop with a minimum of liquid and sealed by placing another 10 μl drop of collagen matrix on the top. Explants were cultured for 24 or 48 h in high glucose DMEM (Gibco) supplemented with 1% FBS (Gibco) and penicillin/streptomycin at 38 °C in CO_2 incubator. Isolated liver buds were cultured with the isolated ductus venosus, the sinus venosus or beads (BIO-RAD). The beads were soaked in PBS containing recombinant human NRTN (1, 25, 50, or 100 ng/ml, PeproTech) or recombinant human GDNF (1, 25, 50, or 100 ng/ml, PeproTech), or 0.1% BSA (SIGMA). Recombinant human GFRα1-Fc and human GFRα2-Fc proteins (R&D Systems, Inc.) were added in to the medium (300 ng/ml).

Results

Ductus venosus secretes a chemoattractant for liver bud

During chick liver development, the liver bud arises from the endoderm of the anterior intestinal portal (AIP), invaginates into the septum transversum mesenchyme (STM) and elongates along the ductus venosus (Romanoff, 1960) (Fig. 1A). In *Flk-1* null mice, which have few endothelial cells (ECs), the liver bud fails to invaginate into the STM and is unable to complete its morphogenetic movement (Matsumoto et al., 2001). This result suggests that ECs play an important role in liver development and further suggests the existence of a soluble factor secreted by ECs that promotes liver bud migration. To examine this possibility, we co-cultured isolated liver buds with either ductus venosus or sinus venosus from HH16–17 chick embryos corresponding to the developmental stage when liver buds are known to migrate along the ductus venosus in intact embryos. After co-culture for 24 h, we observed that the liver bud migrated toward the ductus venosus (Figs. 1B, C; 100%, $n=7/7$) but did not migrate toward the sinus venosus (Figs. 1D, E; 100%, $n=9/9$), suggesting that (a) soluble attractant(s) are secreted from the ductus venosus to promote liver bud migration.

GFRα2 expression in early liver development

Recently, the expression patterns of *GDNF* and its receptors *GFRα1*, *GFRα2*, *GFRα4*, and *c-ret* were described in the chick embryo. *GFRα2* is expressed in the liver (Homma et al., 2000). In addition, *neurturin* (*NRTN*), a ligand for GFRα2, was detected in the hepatic sinusoids of developing mouse embryos and adult mice (Golden et al., 1999). These factors have been reported to play a role in axon guidance and kidney morphogenesis (Sariola and Saarma, 2003), suggesting that they might also play a role in liver development. To examine their role in liver development, we first analyzed the mRNA expression of *GDNF* and its receptors *GFRα1*, *GFRα2*, *GFRα4* and *c-ret* during chick liver development by *in situ* hybridization. At HH22, of these genes we detected the expression of only *GFRα2* in the developing liver (Figs. 2A–E), as previously reported (Homma et al., 2000). The common signaling receptor *c-ret* did not appear to be expressed in the liver, similar to the results of previous studies in the mouse embryo (Golden et al., 1999). Next, we carried out a detailed analysis of the expression pattern of *GFRα2*. *GFRα2* was expressed in the hepatic endoderm and liver bud at a number of developmental stages. These include HH12, at which stage a single layer of the hepatic endoderm is present in the anterior intestinal portal (AIP) (Figs. 2F, G), HH14 and 17, at which stages the liver bud invaginates into the STM and extends in an anterior direction along the ductus venosus, respectively (Figs. 2H–K), HH19, at which stage the elongated liver bud has begun to envelop and form hepatic plates around the ductus venosus (Figs. 2L, M), and HH22, at which stage the hepatic plates have extended radially to form hepatocellular cords (Figs. 2N, O). Transverse sections of each stage indicate that *GFRα2* expression was detected in the hepatic endoderm and hepatic epithelium (Figs. 2P–Q). This expression pattern suggests that *GFRα2* plays a role in liver development.

Isolation of chick NRTN

The chick homolog of NRTN, a specific ligand for GFRα2, has yet to be identified. Thus we first endeavored to clone the

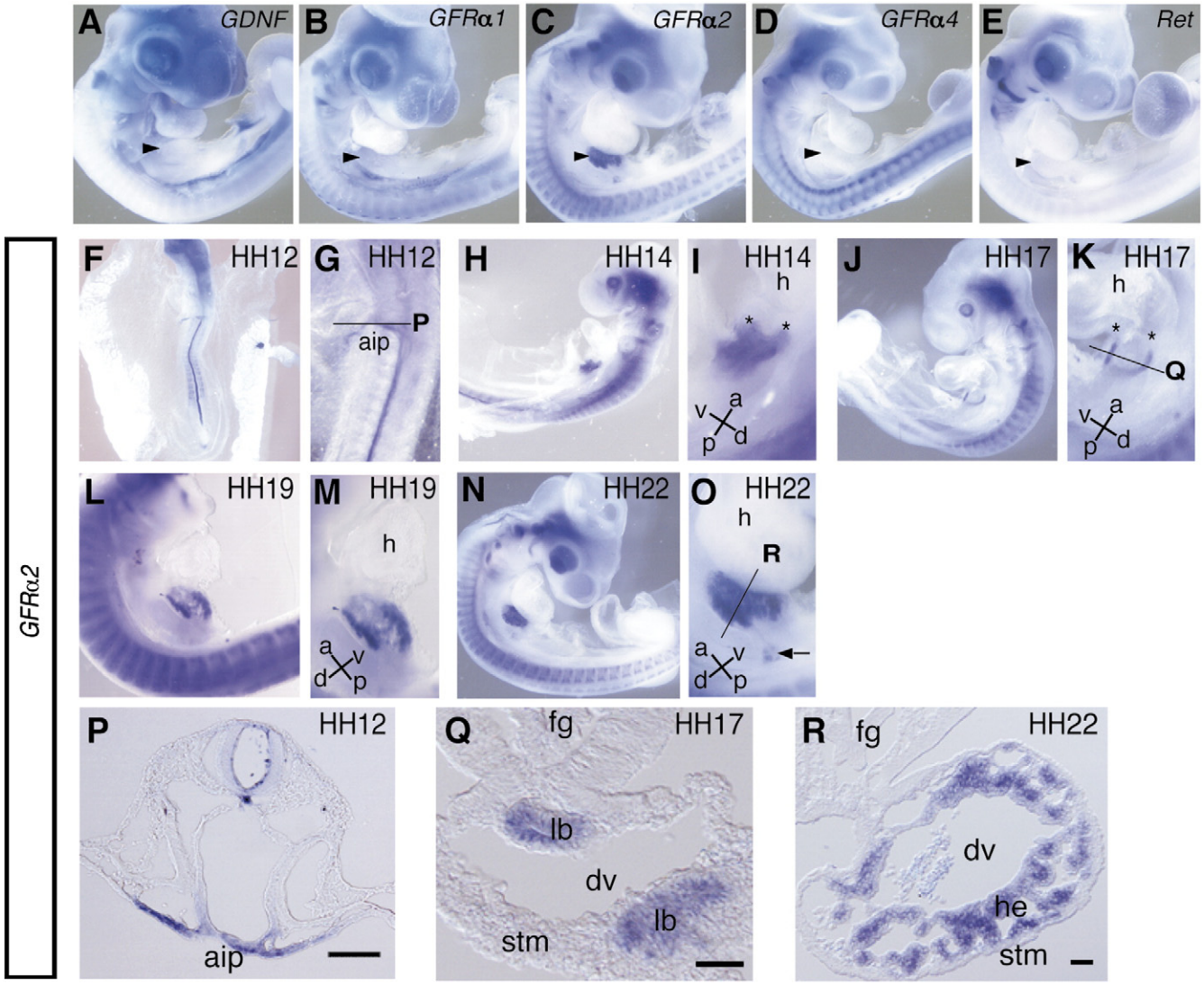

Fig. 2. Expression of *GDNF*-related genes and *GFRα2* in the developing liver. (A–E) Lateral view of whole-mount *in situ* hybridizations of E4 chick embryos with probes for *GDNF* (A), *GFRα1* (B), *GFRα2* (C), *GFRα4* (D), and *c-ret* (E). Arrowheads show the developing liver. (F–R) Expression pattern of *GFRα2* in the hepatic endoderm and hepatic epithelium at different stages of the chick development: HH12 (F, G) 14 (H, I) and 17 (J, K), 19 (L, M), and 22 (N, O). Asterisks show elongating liver buds. Arrow in panel O indicates dorsal pancreas. Panels P, Q, and R show the transverse sections of panels G, K, and O, respectively; The orientation of the embryo is indicated in order to show the direction of the liver bud migration or hepatic epithelium; a, anterior; p, posterior; d, dorsal; v, ventral; aip, anterior intestinal portal; h, heart; fg, foregut; dv, ductus venosus; he, hepatic epithelium; stm, septum transversum mesenchyme. Scale bars are 100 μm.

chick homolog of *NRTN*. We cloned the chick *NRTN* fragment by RT-PCR using degenerate primers derived from a region conserved between the human and mouse *NRTN* genes and chick *GDNF* sequences. The resulting chick *NRTN* fragment was used as a probe to isolate a full-length cDNA from a chick liver library. A full-length clone representing chick *NRTN* (Genbank accession no. AB257073) was isolated and sequenced, revealing an open reading frame of 199 amino acids. The chick NRTN sequence contained a conserved proteolytic cleavage site (RXXR). However, the sequence upstream of the cleavage site exhibited little homology to the corresponding sequences in other vertebrate homologs (Fig. 3A). The predicted amino acid sequence of the mature polypeptide exhibited approximately 69 and 64% similarity to the corresponding sequence of the human and mouse NRTN, respectively (Fig. 3B). There was nearly 45% similarity between the corresponding sequence of the mature chick GDNF and chick NRTN, although the latter also has the conserved seven-cysteine domain of the TGF-β superfamily like the former.

Chick NRTN is expressed in the ductus venosus

A detailed analysis of *NRTN* expression in the mouse embryo and adult mice has previously been reported (Widenfalk et al., 1997; Golden et al., 1999). Mouse *NRTN* transcripts were detected in hepatic sinusoids at E16 and the expression level increased at later stages (Golden et al., 1999). We next analyzed in detail the expression of chick *NRTN* during liver development (Figs. 3C–G). At HH12, *NRTN* mRNA was detected in the endothelium of the vitelline veins lining the hepatic

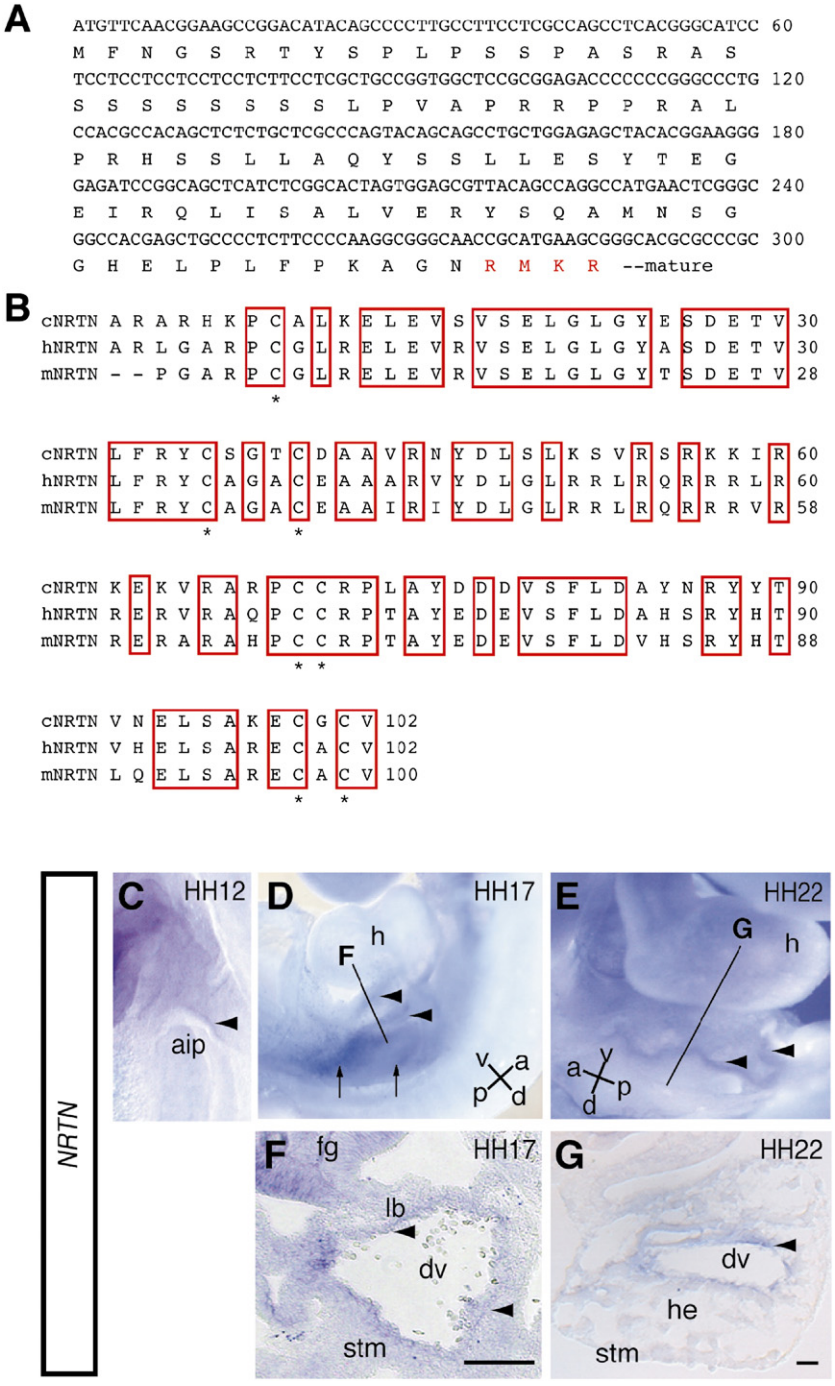

Fig. 3. The predicted amino acid sequence of chick *NRTN* and its expression in developing embryos. (A) The cDNA encoding the N-terminal prodomain. The consensus proteolytic cleavage site for processing (R–X–X–R) is depicted (red text). (B) An alignment of the mature protein sequences of chick (c), human (h), and mouse (m) NRTN. Residues that are identical in the three species are boxed. Asterisks indicate conserved cysteine residues within the TGF-β superfamily. (C–G) The expression of *NRTN*. *NRTN* was detected in the endothelium of the vitelline veins at HH12 (C). At HH17 (D) and HH22 (E), *NRTN* mRNA was detected in the endothelial cells of the ductus venosus (dv). Panels F and G show transverse sections of panels D and E, respectively. Arrowheads indicate endothelial cells expressing *NRTN* and arrows indicate migrating neural crest cells expressing *NRTN* in the foregut mesoderm. The orientation of the embryos is indicated in order to show the direction of the liver bud or hepatic epithelium; a, anterior; p, posterior; d, dorsal; v, ventral; aip, anterior intestinal portal; h, heart; fg, foregut; lb, liver bud; he, hepatic epithelium; stm, septum transversum mesenchyme. Scale bars are 100 μm.

endoderm (Fig. 3C arrowhead). At HH17 and 22, *NRTN* mRNA was detected in the endothelium of the ductus venosus adjacent to the hepatic epithelium but not at the sinus venosus (Figs. 3D–G). Expression was also detected in other tissues, including in migrating neural crest cells in the foregut (Fig. 3D arrows), and in the otic placode, retina, second pharyngeal arch, nephric duct and the limb bud mesenchyme (data not shown). Transverse sections confirmed that the *NRTN* mRNA was localized within the endothelial cells of the ductus venosus (Figs. 3F, G). The simultaneous expression of *NRTN* and

GFRα2 in adjacent tissues suggests that NRTN-GFRα2 signaling might be involved in liver bud migration along the ductus venosus.

Expression of GFRα2-Fc chimera inhibits the elongation of liver bud

To investigate the possibility that NRTN is an attractant for liver bud migration, we constructed a recombinant soluble form of GFRα2 (GFRα2-Fc) fused to the mouse IgG Fc domain at the C-terminal region of GFRα2 from which the GPI-anchoring signal had been removed. We then electroporated the *GFRα2-Fc* chimera into the prospective hepatic endoderm (PHE) of HH12 embryos, to inhibit endogenous signaling by recruiting NRTN and thereby inhibiting its binding to the endogenous receptor. The GFRα1-Fc chimeric protein has already been shown to be effective at inhibiting GDNF-GFRα1 signaling during neurite outgrowth (Mikaels-Edman et al., 2003). At HH12, we electroporated the control plasmid (pCAGGS), pCAGGS-*GFRα2-Fc* or pCAGGS-*GFRα1-Fc* into the PHE along with pCAGGS-*GFP* and the embryos were cultured for either 24 or 48 h. The morphology of the hepatic epithelium was visualized by *in situ* hybridization with the *hhex* probe (a hepatic marker; Yanai et al., 2005) and the distribution of the transgene was identified by co-electroporated GFP (Figs. 4A–F; inset). Twenty-four hours after transfer, expression of *GFRα2-Fc* strongly suppressed the anterior elongation of the liver bud along the ductus venosus (Fig. 4B; 100%, $n=20$) compared to the controls (Fig. 4A; 0%, $n=20$). The mean length of the liver buds of embryos expressing *GFRα2-Fc* was reduced to 22% of that of the controls (Fig. 4G). On the other hand, expression of *GFRα1-Fc*, which can specifically block signaling by GDNF, had no effect on liver bud elongation (Fig. 4C; 100%, $n=20$). These data suggest that only NRTN-GFRα2 signaling is specifically involved in liver bud elongation. To determine whether suppression of elongation was caused by the inhibition of proliferation or by induction of apoptosis, we compared the rates of proliferation and apoptosis in the liver bud of embryos expressing *GFRα2-Fc*

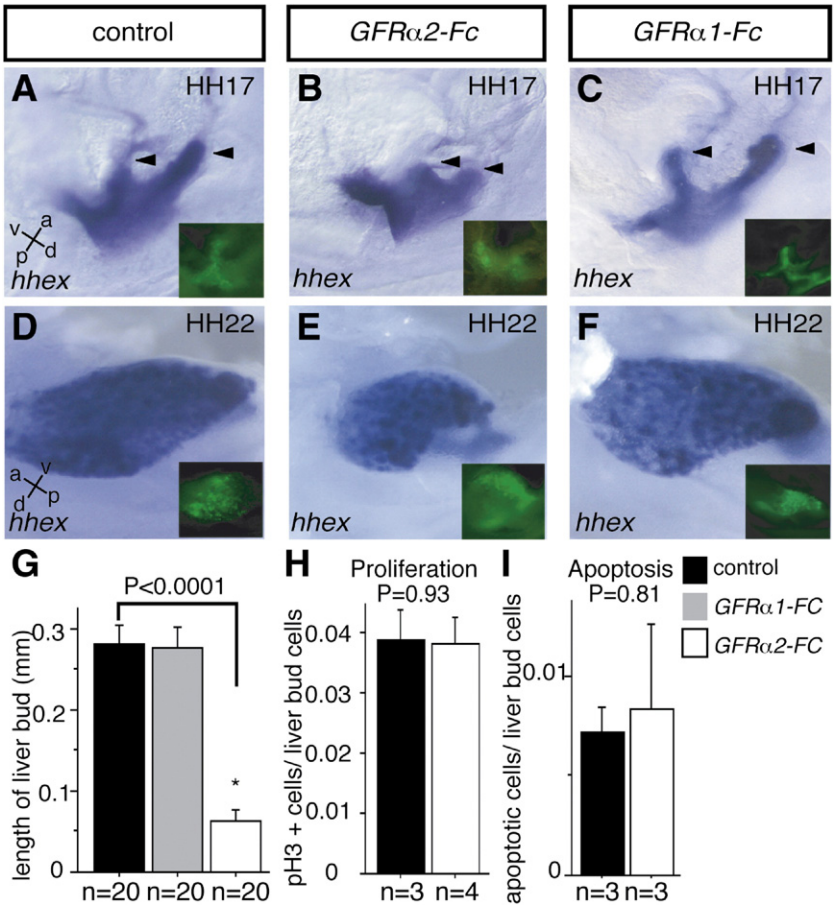

Fig. 4. Expression of *GFRα2-Fc* inhibits liver bud elongation along the ductus venosus. (A–F) The gross morphology of the liver bud (HH17) and liver (HH22) expressing pCAGGS as a control (A, D), pCAGGS-*GFRα2-Fc* (B, E) and pCAGGS-*GFRα1-Fc* (C, F). After culture for 24 or 48 h, the hepatic epithelium of the liver bud or the liver was visualized by whole-mount *in situ* hybridization to an *hhex* probe. Arrowheads show the liver buds. Note that liver bud elongation was inhibited by expression of *GFRα2-Fc* (B). The insets show the distribution of GFP expression as an index of electroporation efficiency. (G) Quantitative analysis of the length of the liver bud along the ductus venosus 24 h after electroporation. (H) The rate of proliferation in liver buds 24 h after electroporation. The fraction of phospho-H3 (pH3) -positive mitotic nuclei in the liver bud. (I) The rate of apoptosis in liver buds 24 h after electroporation. The relative number of apoptotic cells in the liver bud is shown. Closed, shaded, and open bars show the values of the liver buds expressing the control vector, pCAGGS-*GFRα1-Fc* and pCAGGS-*GFRα2-Fc*, respectively. The orientation of the embryos is indicated to show the direction of liver bud migration or hepatic epithelium; a, anterior; p, posterior; d, dorsal; v, ventral.

with the rates observed in the liver bud of control embryos. We found no significant differences in the rate of proliferation or apoptosis between the two embryo groups (Figs. 4H, I). These results suggest that suppression of elongation may be caused by the inhibition of liver bud migration. After culture for 48 h, the inhibition of liver bud elongation caused by *GFRα2-Fc* expression (Fig. 4E; $n=20$) was less dramatic than that observed after culture for 24 h, showing a 30% decline compared with control or *GFRα1-Fc*-expressing embryos (Fig. 4D; $n=20$, F; $n=20$) (data not shown). The expression of other hepatic makers, such as *fibrinogen-γ*, *transthyretin*, *Foxa2* and *Prox1* (Yanai et al., 2005) and *GFRα2*, was unaffected by the expression of *GFRα2-Fc* (data not shown). In addition, to evaluate function of NRTN-GFRα2 signaling at earlier stages of chick liver development, we also introduced *GFRα2-Fc* at HH10, at which time the hepatic endoderm has yet to express GFRα2 mRNA. We then harvested embryos at HH12 and observed no effect on the expression of hepatic markers or on the morphology of the hepatic endoderm (data not shown).

Expression of NRTN perturbs morphogenesis of the liver bud

Next, to elucidate the function of *NRTN* in liver development using a gain-of-function strategy, we electroporated pCAGGS, pCAGGS-*mNRTN*, or pCAGGS-*mGDNF* along with pCAGGS-*GFP* into the prospective hepatic endoderm (PHE) or the prospective midgut endoderm (PME), as chick *NRTN* is expressed in the endothelium of the ductus venosus. After electroporation, the embryos were cultured for either 24 or 48 h to allow the expression of the transgenes. The morphology of the hepatic epithelium was visualized by *in situ* hybridization with the *hhex* probe and the distribution of the transgene was identified by monitoring fluorescence derived from co-electroporated *GFP* (Figs. 5A–F, I, J; inset). The distributions of the genes electroporated into the liver bud are shown in Supplemental Fig. 1. After 24 h in culture, ectopic expression of *mNRTN* in the PME adjacent to the PHE arrested the anterior elongation of the liver bud relative to the control (Fig. 5C; 100%, $n=14$), resulting in liver bud accumulation near the duodenum (Fig. 5D, arrows; 83%, $n=12$), whereas ectopic expression of *mNRTN* in the PHE did not affect liver bud elongation compared to the control (Fig. 5A; 100%, $n=20$, B; 100%, $n=17$). After 48 h in culture, the experimental embryos showed even greater morphological changes. Ectopic expression of mouse NRTN in the PHE suppressed the envelopment of the ductus venosus by the liver bud during HH18–20, resulting in the formation of a split liver (Fig. 5F, dotted area; 73%, $n=15$), compared to the control (Fig. 5E; 100%, $n=15$). Transverse sections of each embryo indicated that the hepatic epithelium ectopically expressing *mNRTN* accumulated on the lateral side of the ductus venosus, whereas the hepatic epithelium completely enveloped the ductus venosus in the control (Figs. 5G, H). Ectopic expression of *mNRTN* in the PME led to the formation of an ectopic branch of the liver bud in the duodenum that did not appear in the control (Fig. 5I; 100%, $n=15$; J arrowheads; 60%, $n=15$). Transverse sections show that *hhex* expression was detected in the duodenum of embryos ectopically expressing *mNRTN* (Fig. 5L), but not in the control (Fig. 5K). The ectopic expression of *mGDNF* in the PHE and PME did not affect morphogenesis of the liver bud (data not shown). These data suggest that NRTN is sufficient to promote the anterior elongation of the liver bud and envelopment of the ductus venosus.

It is possible that ectopic expression of *mNRTN* in the PME may give rise to the formation of an ectopic domain of *hhex*-positive tissue in the duodenum due to ectopic differentiation of the duodenum into *hhex*-positive cells rather than due to abnormal migration of the liver buds. To examine this possibility, PME explants were exposed to recombinant NRTN *in vitro*. However, the hepatic marker *hhex* was not detected in either the control PME explants or explants exposed to NRTN, whereas the definitive endoderm maker *Foxa2* was detected in both control and NRTN-treated explants (Supplemental Fig. 2). This result supports the interpretation that expression of NRTN in the PME did not induce differentiation of PME into hepatic endoderm, but rather that it acted as a chemoattractant for the migrating liver bud *in vivo*.

NRTN is a chemoattractant for liver bud migration

The results reported above strongly suggest that liver bud migration is controlled by GFRα2 and NRTN. An additional possibility is that the migration of the liver bud might be affected by a secondary signal induced by the ectopic expression of NRTN in the surrounding tissues. To demonstrate that NRTN directly promotes the migration of the liver bud, we co-cultured isolated liver buds with beads that had been allowed to absorb growth factor in collagen type I gel (Figs. 6A–C). After 24 h in culture, the liver bud was found to have migrated toward the NRTN-soaked bead (Fig. 6F; 88%, $n=16$). However, in cultures with BSA- or GDNF-soaked bead, the liver bud showed no evidence of migration (Fig. 6D; 100%, $n=12$, E; 100%, $n=9$). We also examined the effect of NRTN and GDNF at several concentrations (1, 25, 50, or 100 ng/ml), and liver bud migration was observed at concentrations of either 50 or 100 ng/ml of NRTN, but not by GDNF at any concentration (data not shown). These results directly demonstrate that NRTN functions as a chemoattractant for liver bud migration.

In addition, to show that GFRα2-Fc specifically inhibits the migration of the liver bud induced by NRTN *in vitro*, we co-cultured liver buds with an NRTN-soaked bead in the presence of no GFRα-Fc, recombinant human GFRα2-Fc or recombinant human GFRα1-Fc. Unexpectedly, we observed that liver buds failed to migrate towards the NRTN-soaked bead when co-cultured in the presence of either GFRα2-Fc or GFRα1-Fc for 24 h, whereas they did migrate in the presence of no GFRα-Fc (data not shown, Figs. 6G and J; 80% $n=5$). The unexpected ability of GFRα1-Fc to inhibit cell migration may be caused by an excess of this soluble receptor fusion, as GFRα1 binds NRTN with low affinity (Klein et al., 1997). After 48 h, little migration of the liver bud towards the NRTN-soaked bead was observed in the presence of GFRα2-Fc (Figs. 6I and L; $n=17$, fraction of migrating buds, 29%) whereas most of the liver buds

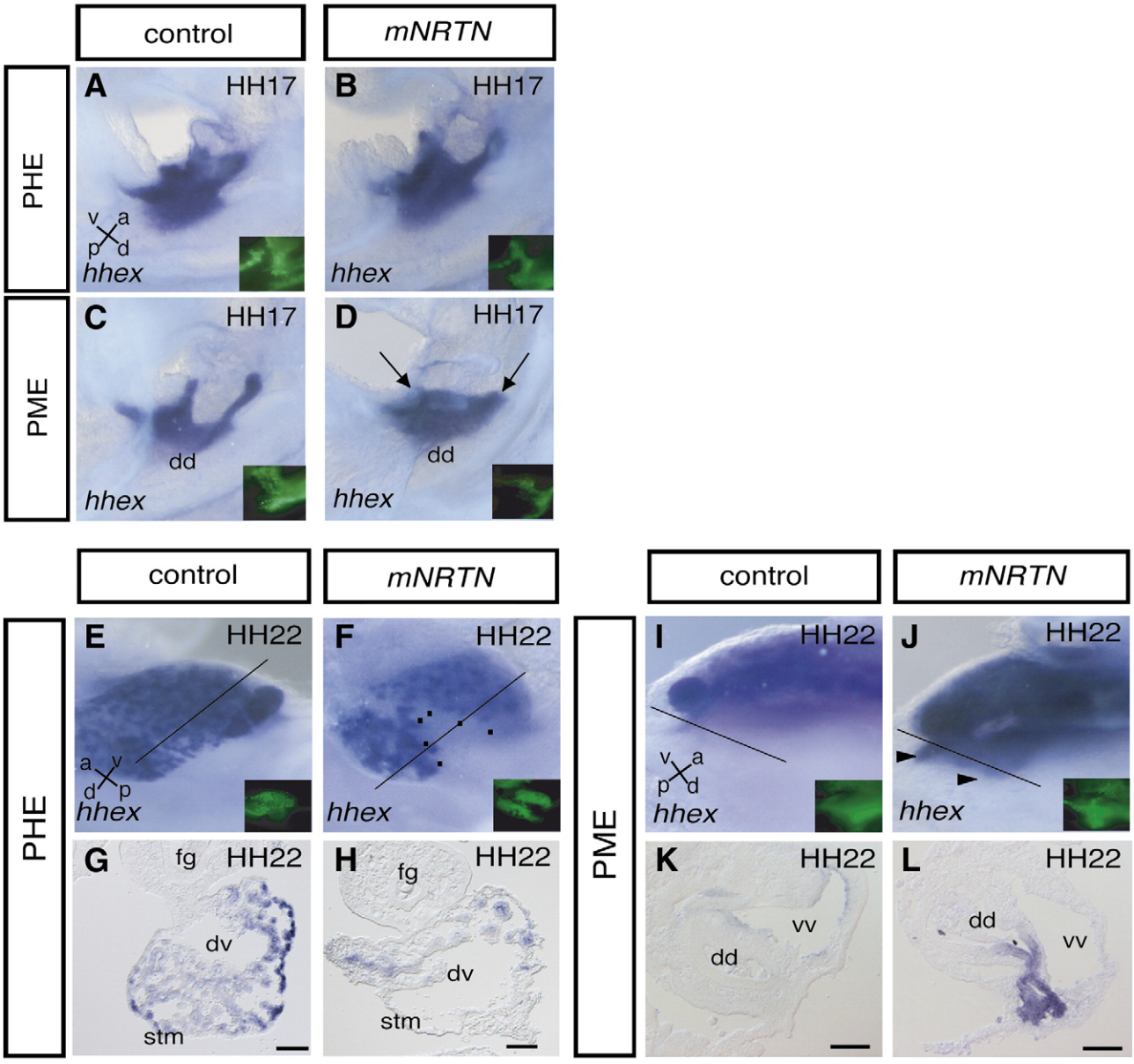

Fig. 5. Ectopic expression of *mNRTN* affects the morphogenesis of the liver (A–L). The gross morphology of the liver bud (HH17) and liver (HH22) in embryos ectopically expressing *mNRTN* in the prospective hepatic endoderm (PHE) (A, B, E, F) or in the prospective midgut endoderm (PME) (C, D, I, J). Following culture for 24 or 48 h, the hepatic epithelium was probed by whole-mount *in situ* hybridization with the *hhex* probe. The inset shows GFP fluorescence monitored as an index of the efficiency of electroporation. (A–D) After 24 h we observed that ectopic expression of *mNRTN* in the PHE did not affect the elongation of the liver bud (B), whereas ectopic expression of *mNRTN* in the PME inhibited anterior elongation of the liver bud (D, arrows). (E, F, I, J) After 48 h, ectopic expression of *mNRTN* in the PHE arrested the envelopment of the liver bud around the ductus venosus, resulting in a split liver (F, dotted area). Ectopic expression of *mNRTN* in the PME induced ectopic branching of the *hhex*-positive tissues in the duodenum (J, arrowheads), but not in controls (I). All controls are developed normally (A, C, E, I). Panels G, H, K, and L are the transverse sections of panels E, F, I, and J, respectively. Orientation of the embryos is indicated in order to show the direction of liver bud migration or hepatic epithelium; a, anterior; p, posterior; d, dorsal; v, ventral; fg, foregut; dd, duodenum; stm, septum transversum mesenchyme; dv, ductus venosus; vv, vitelline vein. Scale bars are 100 μm.

incubated in the presence of GFRα1-Fc migrated successfully to the NRTN-soaked bead (Figs. 6H and K; fraction of migrating buds, 78% $n=18$). These results indicate that GFRα2-Fc specifically inhibits the migration of the liver bud induced by NRTN *in vitro*.

During HH14–17 in chick embryos, the liver bud selectively elongates in an anterior direction despite the fact that *NRTN* is ubiquitously expressed in the endothelial cells of the ductus venosus and *GFRα2* is expressed throughout the liver bud. Localization of responsiveness to NRTN in the migrating liver bud might explain this apparent inconsistency between the pattern of gene expression and directional elongation of the liver bud. To investigate this possibility, we placed an NRTN-soaked bead at different positions around the liver bud *in vitro*. However, the frequency of the migration was not influenced by the position of the bead (data not shown).

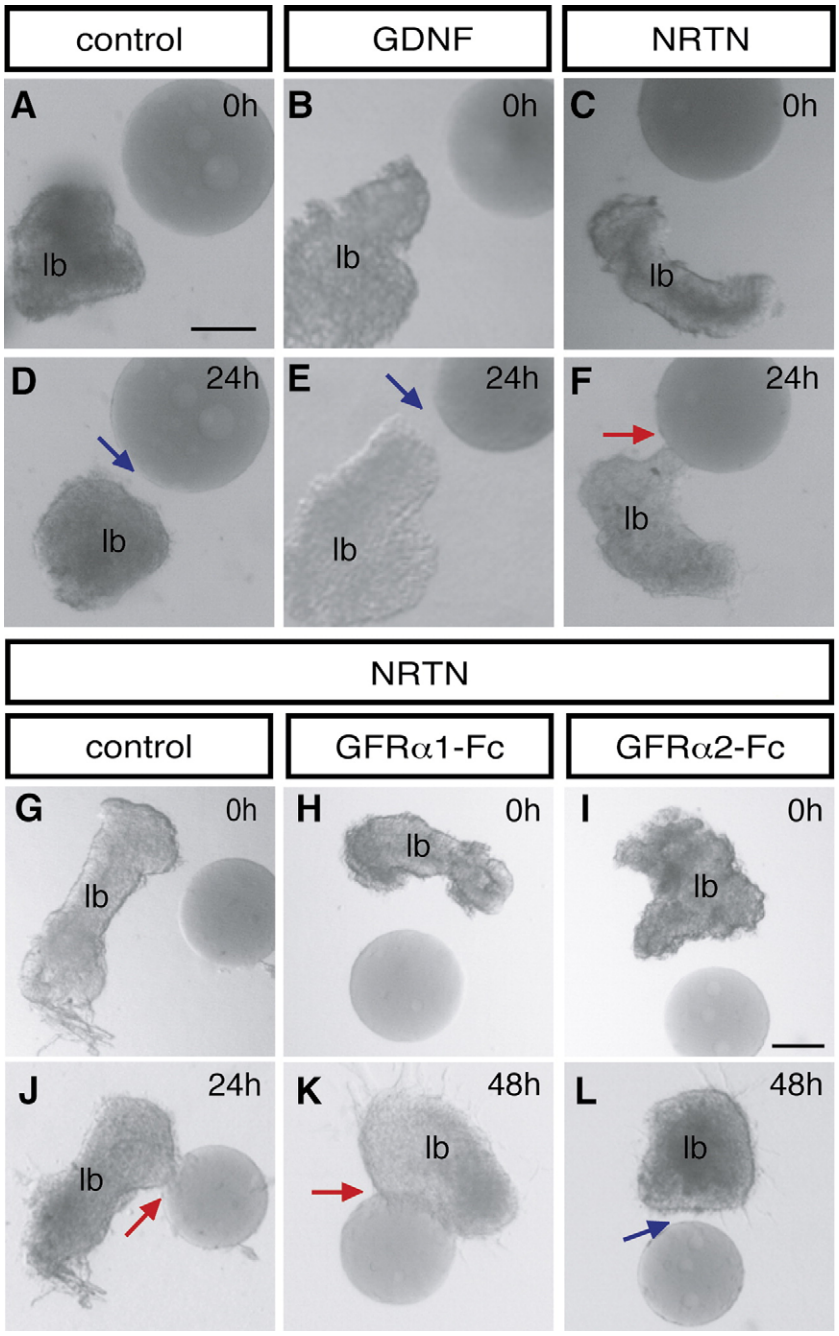

Fig. 6. NRTN acts as a chemoattractant for the liver bud *in vitro*. (A–F) Isolated liver buds (lb) from HH16 chick embryos were cultured for 24 h in a collagen gel with beads soaked in BSA as a control (A, D), in GDNF (B, E), or in NRTN (C, F). (G–L) Isolated liver buds from HH16 chick embryo were cultured with beads soaked NRTN for 24–48 h in a collagen gel and medium containing no GFRα-Fc (G, J), GFRα1-Fc (H, K), or GFRα2-Fc (I, L). The red arrow in panels F, J and K shows the liver bud migrating toward the NRTN-soaked bead. The blue arrows in panels D, E and L show the gaps between the liver buds. Scale bars are 100 μm.

Distribution of the basement membrane in the chick liver bud

As shown previously, chick liver buds extend in particular directions depending on the developmental stage, although both the ligand *NRTN* and the receptor *GFRα2* are ubiquitously distributed in the endothelium of the ductus venosus and the liver buds, respectively (Figs. 2 and 3).

It has been reported that the degradation of the basement membrane beneath the mouse liver bud is involved in the delamination of the hepatocyte from the hepatic epithelium (Sosa-Pineda et al., 2000; Shiojiri and Sugiyama, 2004; Bort et al., 2006). Therefore, we evaluated the distribution of laminin and E-cadherin using immunohistochemistry to determine whether there is a correlation between the directional morphogenesis of the chick liver bud and the distribution of the basement membrane. Laminin is a major component of the basement membrane and E-cadherin is a marker for hepatic epithelium at early developmental stages. At HH 14, when the

hepatic epithelium begins to invaginate into the septum transversum, the liver bud is surrounded by the basement membrane (data not shown). At HH 16, when the liver bud has extended in an anterior direction on the ductus venosus, the anterior tips of the liver buds were locally laminin-negative (Figs. 7A, A′ arrowhead). At HH 18, when the liver buds have extended laterally on the ductus venosus, the lateral edges of the extending liver buds were locally laminin-negative (Figs. 7B, B′ arrowhead). These results suggest that there is a correlation between the directional morphogenesis of the liver buds and the degradation pattern of laminin.

In addition, to test whether local degradation of the basement membrane is regulated by NRTN-GFRα2 signaling, we investigated the effect of expression of GFRα2-Fc on the

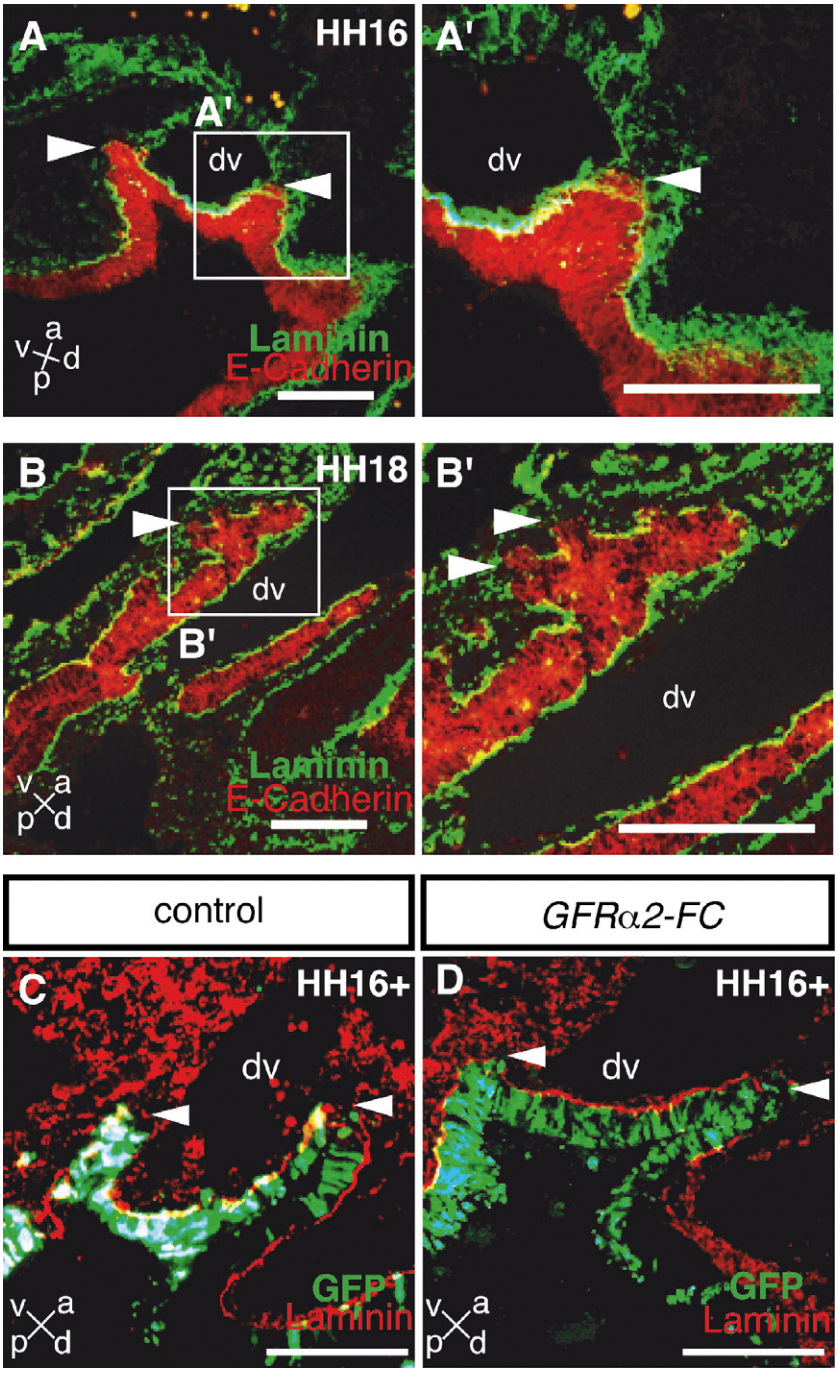

Fig. 7. Distribution of the basement membrane around the liver bud in the HH16 and HH18 chick embryo. (A, B) Sagittal sections of HH16 and HH18 liver buds. (A′, B′) High-power magnifications of the same sections. The image of the liver bud detected by immunostaining for E-cadherin (red) and that of basement membrane detected by immunostaining for laminin (green) were merged (A, B). (C, D) A sagittal section of HH16+ liver buds electroporated with transgenes. Distribution of the transgenes was monitored by GFP immunofluorescence (green) and that of the basement membrane was detected by laminin immunofluorescence (red). (C) Control embryo and (D) embryos expressing GFRα2-Fc. Arrowheads show the degradation of laminin. dv, Ductus venosus. The orientation of the embryos is indicated in order to show the direction of liver bud migration; a, anterior; p, posterior; d, dorsal; v, ventral. Scale bars are 100 μm.

distribution of laminin at HH16+ when the liver buds extend towards the anterior. As shown previously, forced expression of GFRα2-Fc arrested the anterior elongation of the liver bud. However, it did not affect the distribution of laminin (Figs. 7C, D arrowhead). This result suggests that NRTN-GFRα2 signaling is not involved in the regulation of the local degradation of the basement membrane.

Discussion

Liver bud migration is an important event for normal liver development. The mouse liver bud undergoes several independent morphogenetic processes: invagination, delamination, migration, and proliferation (Lemaigre and Zaret, 2004; Zhao and Duncan, 2005; Bort et al., 2006). In the chick liver bud, the migration process can be divided into two sub-processes: anterior elongation and the envelopment of the ductus venosus (Romanoff, 1960). However, the molecular mechanisms of these processes, in particular the interaction of the liver bud with the surrounding tissues, are poorly understood. In this study, we have found that the ductus venosus secretes a soluble factor that promotes migration of the liver bud. We also showed that *neurturin* (*NRTN*) and its receptor *GFRα2* are expressed in the endothelium of the ductus venosus and in the liver bud, respectively. We further demonstrated that NRTN acts as a chemoattractant for liver bud expressing GFRα2 in reminiscent of the role of NRTN in neuronal migration both *in vivo* and *in vitro* (Yan et al., 2004).

NRTN-GFRα2 signaling directly controls the migration of the liver bud

We observed that expression of *GFRα2-Fc* inhibits the elongation of the liver bud along the ductus venosus (Fig. 4B). However, we did not observe any effects on cell proliferation, apoptosis, or the expression of hepatic markers in the liver bud (Figs. 4H, I and data not shown). These results suggest that NRTN-GFRα2 signaling directly controls the migration of the liver bud without affecting proliferation, apoptosis, or differentiation. In addition, we found the rate of cell proliferation in the migrating liver bud was originally very low (Fig. 4H). Moreover, DAPI staining of the liver bud revealed that endodermal cells in the hepatic diverticula are randomly packed at high cell density before invagination, whereas epithelial cells in the migrating liver bud are evenly aligned (data not shown). This observation suggests that liver bud invagination might partially involve a mechanism similar to that observed during convergent extension cell movement during gastrulation (Gerhart and Keller, 1986).

Ectopic expression of *NRTN* demonstrated that the resulting phenotypes depend on the location of the gene transfer. Ectopic expression of *NRTN* in the PHE prevented the liver bud from enveloping the ductus venosus (Fig. 5F), whereas ectopic expression of *NRTN* in the PME induced the ectopic branching of a liver bud in the duodenum (Fig. 5J). These data suggest that normal distribution of NRTN is crucial for the proper morphogenesis of the liver bud. Moreover, we observed local degradation of laminin in the tips of the migrating liver bud (Fig. 7). This result suggests that in the chick embryo, degradation of the basement membrane of the liver bud might be involved in the migration into the STM, as occurs during development of the murine liver (Sosa-Pineda et al., 2000).

NRTN-GFRα2 signaling is mediated by a RET-independent pathway

The intracellular signaling by the GFL-GFRα complex is mediated predominantly by the RET tyrosine kinase (Sariola and Saarma, 2003). However, the chick liver bud and liver do not express *c-ret* during the HH11 to HH24 developmental stages. Likewise, the mouse embryonic liver does not express *c-ret* at comparable developmental stages (Golden et al., 1999). These data suggest that signaling by the NRTN-GFRα2 complex is mediated by a RET-independent pathway in the developing liver. As NCAM is reported to function as an alternative signaling receptor for the GDNF-GFRα1 complex in neuronal cells (Paratcha et al., 2003), we analyzed the expression of NCAM in the migrating chick liver bud by *in situ* hybridization, but we could not detect it (data not shown). This suggests that other, as yet unknown, signaling molecules are required for the intracellular signaling by the NRTN-GFRα2 complex in the developing liver.

The effective distance of NRTN diffusion

To estimate the effective range of the diffusion of NRTN *in vivo*, we co-cultured the liver bud with an NRTN-soaked bead (50 ng/ml) placed at different distances from the liver bud. We found that the effective range of NRTN action was approximately 40–80 μm (data not shown). The effective range for the diffusion of FGF10 for the lung bud is 150 μm (Weaver et al., 2000). Moreover, the effective concentration of NRTN was greater than 50 ng/ml when the distance of the bead from the liver bud was fixed at 40–60 μm (data not shown). Our *in vivo* data are consistent with these results. We observed induction of ectopic liver bud formation into the PME when *NRTN* was ectopically expressed in the vicinity of the liver bud (Fig. 5J), but we did not observe any ectopic liver bud formation when *NRTN* was expressed distally from the liver bud (data not shown). These results also suggest that the distance between the GFRα2-expressing liver bud and *NRTN*-expressing endothelial cells of the ductus venosus is important to the liver bud migration.

GFLs have also been reported to interact with the heparan-sulphate side chains of extracellular matrix proteoglycans, which might restrict their diffusion and raise their local concentration (Hamilton et al., 2001). These data suggest that close proximity of the NRTN-expressing tissue and a high level of NRTN concentration are required for the induction of liver bud migration *in vivo*.

Determination of the direction of liver bud migration

We found that there was a discrepancy between the pattern of *NRTN* and *GFRα2* expression and the directional guidance of

liver bud morphogenesis. Although *NRTN* and *GFRα2* are homogenously expressed in the ductus venosus and in the liver bud respectively, during HH15–17, the liver bud extends solely in an anterior direction. Subsequently, during HH17–21, it extends laterally to envelop the ductus venosus (Figs. 2F–O). These observations suggest that a mechanism exists to control the localization of the responsiveness to NRTN. However, an NRTN-soaked bead placed in any position was able to induce the migration of the liver bud *in vitro* (data not shown), suggesting that all regions of the liver bud possess the capacity to respond NRTN.

These results raise the question of what factor(s) determine (s) the direction of liver bud migration. One possibility is that the distribution of the basement membrane might be involved in the determination of the direction of liver bud migration because it has been reported that the degradation of the basement membrane appears to be involved in the migration of mouse hepatocytes (Sosa-Pineda et al., 2000). In this study, we found that laminin was locally degraded in the basement membrane of the anterior tips of the liver bud at HH16 (Figs. 7A, A′) and in the lateral tips at HH18 (Figs. 7B, B′), which corresponded to the directions of the migration of the liver buds. These observations suggest that distribution of the basement membrane might regulate the direction of liver bud migration.

We also examined whether degradation of the laminin was controlled by NRTN-GFRα2 signaling. However, we did not observe degradation of laminin in response to forced expression of GFRα2-Fc (Fig. 7D). This observation suggests that liver bud migration is regulated by multiple factors, and not by any single factor. These factors include chemoattractants, like NRTN, which induce the liver bud to migrate. In addition, the distribution of basement membrane components, such as laminin, can also provide signals that cue the direction of liver bud migration. In other words, the accessibility of the chemoattractant to the liver bud may be controlled by the degradation pattern of the basement membrane. Clarifying how the basement membrane influences liver bud migration should allow for a better understanding the process that regulates migration of the liver bud.

A model for the migrating liver bud

We first outline current evidence used to establish a proposed model for liver bud migration (Fig. 8). Firstly, *NRTN* is expressed in all endothelial cells lining the ductus venosus from HH12 to HH22. Secondly, all hepatoblasts of the migrating liver bud express *GFRα2*, the specific receptor for NRTN, at the corresponding developmental stages. Finally, NRTN functions an attractant for liver bud migration *in vivo* and *in vitro*. Based on this evidence, we propose a model to explain the complex migration process of the liver bud along the ductus venosus in the chick embryo. During HH12–14, *NRTN* and *GFRα2* have already been expressed in the hepatic endoderm and the vitelline vein, respectively. During HH15–17, the two liver buds invade the septum transversum mesenchyme. Then, liver buds migrate in an anterior direction along the ductus venosus

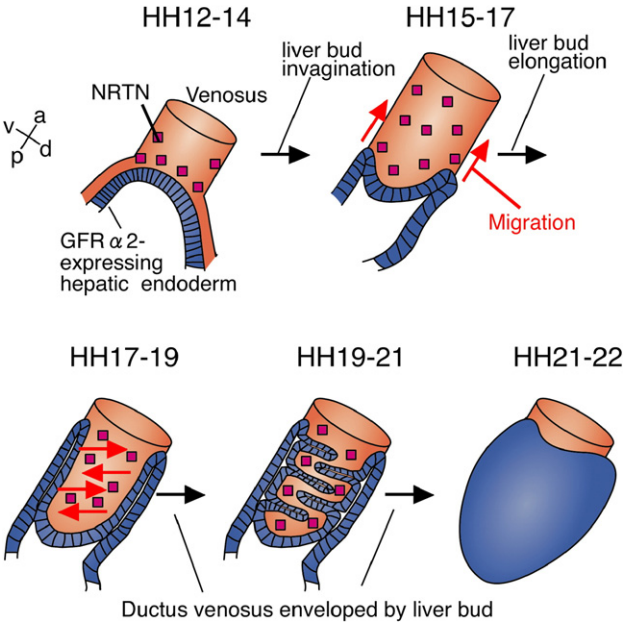

Fig. 8. Model of NRTN-GFRα2 signaling in the migrating liver bud. During early liver development, NRTN (purple) secreted from the endothelium of the ductus venosus (red) chemically attracts the movement of the liver bud (blue) expressing *GFRα2* in each stage.

using NRTN as the chemoattractant. During HH17–19, the liver buds migrate laterally on the ductus venosus, and finally envelop it in HH19–21.

The critical developmental stages of NRTN-GFRα2 signaling

In this report, we have shown that at stage 12, the hepatic endoderm in the anterior intestinal portal and the adjacent endothelium begin to express *GFRα2* and *NRTN*, respectively, and that the expressions of *NRTN* and *GFRα2* are maintained subsequently in derivative tissues (ECs of the DV and liver buds, respectively) (Figs. 2 and 3). This finding raises the question of when NRTN-GFRα2 signaling is required for liver development.

The results reported here suggest that the first critical stage would be between HH 15 and 17 when the liver buds extend in an anterior direction on the ductus venosus. Consistent with this, we observed arrest of liver bud extension at HH 16–17 in response to expression of GFRα2-Fc (Fig. 4B). A second critical period for NRTN-GFRα2 signaling appears to be HH 17–21 when the liver buds envelop the ductus venosus. Consistent with this, we observed that ectopic expression of NRTN in the liver bud perturbed the envelopment of the ductus venosus, resulting in a split liver at HH 22 (Fig. 5F). Furthermore, we observed that HH 17 liver buds extend towards a source of NRTN *in vitro* (Figs. 6C, F).

Although we have shown here that NRTN-GFRα2 signaling is required for early liver morphogenesis, we have yet to examine a role for such signals at later stages. Therefore, we cannot rule out a role for NRTN-GFRα2 signaling in later stages of chick liver development.

Is NRTN-GFRα2 signaling required for migration of mouse hepatoblasts?

In this study, we found that the migration of the chick liver bud along the ductus venosus is controlled by the chemoattractant NRTN, raising the question as to whether such signaling plays a role in the development of the mouse liver. It is difficult to demonstrate that this signaling pathway is involved in the migration of mouse hepatoblasts, because the venous systems crucial for early liver bud mophogenesis differ in chick and mouse development. During chick liver development, the ductus venosus plays a central role as a scaffold for the morphogenesis of the liver bud. The liver buds extend forward and laterally on the ductus venosus and finally envelop it (Romanoff, 1960; Le Douarin, 1975). On the other hand, during mouse liver bud migration, scattered endothelial cells in the STM surround the liver bud instead of the ductus venosus and the migration of hepatoblasts depends on these endothelial cells but the ductus venosus (Matsumoto et al., 2001).

It remains possible that the scattered endothelial cells in the mouse STM might express NRTN and thereby control mouse hepatoblast migration. But, analysis of the expression patterns of mouse *NRTN* and *GFRα2* suggests that signaling by these factors might not be involved in the mouse liver. Whereas the migration of mouse hepatoblasts into the STM occurs from E9.0, the expression of *NRTN* and *GFRα2* in the mouse liver is only detected at E12 and E16, respectively (Golden et al., 1999). Expression of *NRTN* has also been detected in the hepatic sinusoids at E16 (Golden et al., 1999). To confirm this observation, we performed RT-PCR analysis on RNA isolated from mouse hepatoblasts at E9.5, E12.5, and E14.5 and only detected the expression of *GFRα2* mRNA from stage E12.5 onwards (data not shown). These results suggest that NRTN-GFRα2 signaling does not contribute to the migration of the liver bud during mouse liver development.

These findings suggest that a chemoattractant factor other than NRTN, and emanating from endothelial cells in the mouse STM, may control mouse hepatoblast migration. Identifying this unknown molecule(s) is important for a better understanding of mouse hepatoblast migration.

An additional question is the role of NRTN following the hepatoblast migration stage. It is possible that signaling by NRTN-GFRα2 in mouse embryonic liver might be important for the proper assembly of sinusoidal endothelial cells and the hepatic endoderm after E12.5. We also observed the expression of GFRα2 and NRTN in hepatoblasts and the endothelial cells of the ductus venosus, and of sinusoids in the livers of 7-day-old chicks (Supplemental Figs. 3A, B, B′ and C). These results suggest that NRTN-GFRα2 signaling plays a similar role after the migration stages in both the chick and mouse.

Conclusion

In this study we have shown that the morphogenetic movement of the liver bud is controlled by a chemoattractant ligand expressed by endothelial cells on the ductus venosus. The findings reported here should prove useful for the development of methods for the three-dimensional arrangement of hepatoblasts *in vitro* with a view to their application in regenerative medicine. In addition, we detected the expression of *GFRα2* mRNA not only in the liver but also in the developing ventral and dorsal pancreas. In vertebrates, the pancreas arises from two separate buds (the ventral and dorsal pancreatic buds) that fuse to form the pancreas after the rotation of the duodenum (Moore and Persaud, 1998; Romanoff, 1960). This suggests that NRTN-GFRα2 signaling is not only involved in the migration of the liver bud but also might be involved in the pancreatic buds development. The findings here represent the first functional analysis of GDNF-related factors in the development of endodermal tissues.

Acknowledgments

We greatly appreciate Dr. K. Zaret for the good discussion and pieces of advice. We thank Drs. S. Homma, F. Costantini, and W. J. LaRochelle for kindly providing the plasmids containing chick *GFRα1*, *GFRα2* and *GDNF*, *c-ret* proto-oncogene, La518 Fc vector. We also thank J. Kusuura, J. Okada, M. Iimori, and I. Matsuyama for their technical support and Drs. K. Matsumoto, M. Nakayama and M. Yanai for their technical advice and discussion. This work was mainly supported by a Grant-in-Aid for Scientific Research from the Japan Society for the Promotion of Science; a Grant-in-Aid for Scientific Research from the Ministry of Education, Science, Sports and Culture of Japan to Y.Y., in part by Grants-in-Aid for 21st Century COE Research from the Ministry of Education, Culture, Sports, Science and Technology ‘Cell Fate Regulation Research and Education Unit’, and Institute of Resource Development and Analysis Radioisotope Center.

Appendix A. Supplementary data

Supplementary data associated with this article can be found, in the online version, at doi:10.1016/j.ydbio.2007.03.519.

References

Airaksinen, M.S., Saarma, M., 2002. The GDNF family: signalling, biological functions and therapeutic value. Nat. Rev. Neurosci. 3, 383–394.

Bort, R., Signore, M., Tremblay, K., Martinez Barbera, J.P., Zaret, K.S., 2006. *Hex* homeobox gene controls the transition of the endoderm to a pseudostratified, cell emergent epithelium for liver bud development. Dev. Biol. 290, 44–56.

Burke, Z., Oliver, G., 2002. *Prox1* is an early specific marker for the developing liver and pancreas in the mammalian foregut endoderm. Mech. Dev. 118, 147–155.

Flamme, I., 1987. Prolonged and simplified *in vitro* culture of explanted chick embryos. Anat. Embryol. (Berl.) 176, 45–52.

Gerhart, J., Keller, R., 1986. Region-specific cell activities in amphibian gastrulation. Annu. Rev. Cell Biol. 2, 201–229.

Golden, J.P., DeMaro, J.A., Osborne, P.A., Milbrandt, J., Johnson Jr., E.M., 1999. Expression of *neurturin*, *GDNF*, and *GDNF* family-receptor mRNA in the developing and mature mouse. Exp. Neurol. 158, 504–528.

Hamburger, V., Hamilton, H.L., 1951. A series of normal stages in the development of the chick embryo. J. Morphol. 88, 49–92.

Hamilton, J.F., Morrison, P.F., Chen, M.Y., Harvey-White, J., Pernaute, R.S.,

Phillips, H., Oldfield, E., Bankiewicz, K.S., 2001. Heparin coinfusion during convection-enhanced delivery (CED) increases the distribution of the glial-derived neurotrophic factor (GDNF) ligand family in rat striatum and enhances the pharmacological activity of neurturin. Exp. Neurol. 168, 155–161.

Hentsch, B., Lyons, I., Li, R., Hartley, L., Lints, T.J., Adams, J.M., Harvey, R.P., 1996. *Hlx* homeobox gene is essential for an inductive tissue interaction that drives expansion of embryonic liver and gut. Genes Dev. 10, 70–79.

Hinck, L., 2004. The versatile roles of "axon guidance" cues in tissue morphogenesis. Dev. Cell 7, 783–793.

Homma, S., Oppenheim, R.W., Yaginuma, H., Kimura, S., 2000. Expression pattern of *GDNF*, *c-ret*, and *GFRαs* suggests novel roles for GDNF ligands during early organogenesis in the chick embryo. Dev. Biol. 217, 121–137.

Jung, J., Zheng, M., Goldfarb, M., Zaret, K.S., 1999. Initiation of mammalian liver development from endoderm by fibroblast growth factors. Science 284, 1998–2003.

Kaufman, H.M., Bard, B.L.J., 1999. The Anatomical Basis of Mouse Development. Academic Press, San Diego, CA.

Klein, R.D., Sherman, D., Ho, W.H., Stone, D., Bennett, G.L., Moffat, B., Vandlen, R., Simmons, L., Gu, Q., Hongo, J.A., Devaux, B., Poulsen, K., Armanini, M., Nozaki, C., Asai, N., Goddard, A., Phillips, H., Henderson, C. E., Takahashi, M., Rosenthal, A., 1997. A GPI-linked protein that interacts with Ret to form a candidate neurturin receptor. Nature 387, 717–721.

LaRochelle, W.J., Dirsch, O.R., Finch, P.W., Cheon, H.G., May, M., Marchese, C., Pierce, J.H., Aaronson, S.A., 1995. Specific receptor detection by a functional keratinocyte growth factor-immunoglobulin chimera. J. Cell Biol. 129, 357–366.

Laufer, E., Dahn, R., Orozco, O.E., Yeo, C.Y., Pisenti, J., Henrique, D., Abbott, U.K., Fallon, J.F., Tabin, C., 1997. Expression of radical fringe in limb-bud ectoderm regulates apical ectodermal ridge formation. Nature 386, 366–373.

Le Douarin, N.M., 1975. An experimental analysis of liver development. Med. Biol. 53, 427–455.

Ledda, F., Paratcha, G., Ibanez, C.F., 2002. Target-derived *GFRα1* as an attractive guidance signal for developing sensory and sympathetic axons via activation of *Cdk5*. Neuron 36, 387–401.

Lemaigre, F., Zaret, K.S., 2004. Liver development update: new embryo models, cell lineage control, and morphogenesis. Curr. Opin. Genet. Dev. 14, 582–590.

Liu, Y.W., Gao, W., Teh, H.L., Tan, J.H., Chan, W.K., 2003. *Prox1* is a novel coregulator of *Ff1b* and is involved in the embryonic development of the zebrafish interrenal primordium. Mol. Cell Biol. 23, 7243–7255.

Matsumoto, K., Yoshitomi, H., Rossant, J., Zaret, K.S., 2001. Liver organogenesis promoted by endothelial cells prior to vascular function. Science 294, 559–563.

Matsushita, S., 1999. Fate mapping study of the endoderm in the posterior part of the 1.5-day-old chick embryo. Dev. Growth Differ. 41, 313–319.

Mikaels-Edman, A., Baudet, C., Ernfors, P., 2003. Soluble and bound forms of GFRα1 elicit different GDNF-independent neurite growth responses in primary sensory neurons. Dev. Dyn. 227, 27–34.

Moore, KL., Persaud, T.V.N., 1998. The Developing Human: Clinically Oriented Embryology, 6th edition. W.B. Saunders, Philadelphia.

Niwa, H., Yamamura, K., Miyazaki, J., 1991. Efficient selection for high-expression transfectants with a novel eukaryotic vector. Gene 108, 193–199.

Nogawa, H., Ito, T., 1995. Branching morphogenesis of embryonic mouse lung epithelium in mesenchyme-free culture. Development 121, 1015–1022.

Paratcha, G., Ledda, F., Ibanez, C.F., 2003. The neural cell adhesion molecule NCAM is an alternative signaling receptor for GDNF family ligands. Cell 113, 867–879.

Riddle, R.D., Johnson, R.L., Laufer, E., Tabin, C., 1993. Sonic hedgehog mediates the polarizing activity of the ZPA. Cell 75, 1401–1416.

Romanoff, A.L., 1960. The Avian Embryo: Structural and Functional Development. The Macmillan Company, New York.

Rossi, J.M., Dunn, N.R., Hogan, B.L., Zaret, K.S., 2001. Distinct mesodermal signals, including BMPs from the septum transversum mesenchyme, are required in combination for hepatogenesis from the endoderm. Genes Dev. 15, 1998–2009.

Sariola, H., Saarma, M., 2003. Novel functions and signalling pathways for GDNF. J. Cell Sci. 116, 3855–3862.

Schuchardt, A., Srinivas, S., Pachnis, V., Costantini, F., 1995. Isolation and characterization of a chicken homolog of the *c-ret* proto-oncogene. Oncogene 10, 641–649.

Shiojiri, N., Sugiyama, Y., 2004. Immunolocalization of extracellular matrix components and integrins during mouse liver development. Hepatology 40, 346–355.

Sosa-Pineda, B., Wigle, J.T., Oliver, G., 2000. Hepatocyte migration during liver development requires *Prox1*. Nat. Genet. 25, 254–255.

Weaver, M., Dunn, N.R., Hogan, B.L., 2000. *Bmp4* and *Fgf10* play opposing roles during lung bud morphogenesis. Development 127, 2695–2704.

Widenfalk, J., Nosrat, C., Tomac, A., Westphal, H., Hoffer, B., Olson, L., 1997. Neurturin and glial cell line-derived neurotrophic factor receptor-beta (GDNFR-β), novel proteins related to GDNF and GDNFR-α with specific cellular patterns of expression suggesting roles in the developing and adult nervous system and in peripheral organs. J. Neurosci. 17, 8506–8519.

Yan, H., Bergner, A.J., Enomoto, H., Milbrandt, J., Newgreen, D.F., Young, H.M., 2004. Neural cells in the esophagus respond to glial cell line-derived neurotrophic factor and neurturin, and are RET-dependent. Dev. Biol. 272, 118–133.

Yanai, M., Tatsumi, N., Endo, F., Yokouchi, Y., 2005. Analysis of gene expression patterns in the developing chick liver. Dev. Dyn. 233, 1116–1122.

Yokouchi, Y., 2005. Establishment of a chick embryo model for analyzing liver development and a search for candidate genes. Dev. Growth Differ. 47, 357–366.

Zaret, K.S., 1996. Molecular genetics of early liver development. Annu. Rev. Physiol. 58, 231–251.

Zhao, R., Duncan, S.A., 2005. Embryonic development of the liver. Hepatology 41, 956–967.